Journal of Pharmacognosy and Phytochemistry
Available online at www.phytojournal.com

E-ISSN: 2278-4136
P-ISSN: 2349-8234
www.phytojournal.com
JPP 2024; 13(4): 223-233
Received: 05-06-2024
Accepted: 02-07-2024

Aswini M
Ph.D., Research scholar, Department of Biotechnology, PSG College of Arts & Science, Coimbatore, Tamil Nadu, India

Dr. S Kavitha Bagya
Associate Professor, Department of Biotechnology, PSG College of Arts & Science, Coimbatore, Tamil Nadu, India

Corresponding Author:
Aswini M
Ph.D., Research Scholar, Department of Biotechnology, PSG College of Arts & Science, Coimbatore, Tamil Nadu, India

Prediction and investigation of prognostic factors, therapeutic targets from medicinally significant plant for breast cancer

Aswini M and Dr. S Kavitha Bagya

DOI: https://doi.org/10.22271/phyto.2024.v13.i4c.15013

Abstract
Breast cancer is the 2nd leading cause of mortality and frequently diagnosed malignancy. BCL2 is unregulated by the hormone oestrogens through a direct consequence of transcriptional induction. Components of medicinal plants can be searched for potent therapeutic protein targets, active sites, and significant hits that will be further studied in lead optimisation and drug development to offer computational support for creating pharmaceuticals. *In-silico* study tools help to predict the active drug candidate and forecast oral bioavailability to construct suitable invigorating approaches to superintend human cancer effects. Despite some promising results in examining inhibitory mechanisms, and safety efficacy treatment, both *In-silico* and invitro approaches to search for suitable drugs from the FDA-approved drug library. In this study of Phyto lipids 17-phenyl-omega-trinor-PGE2, (2E, 4E, 8E, 10E)-dodecatetraenedioic acid, Pentanamide 3-oxo-N-[(3S)-tetrahydro-2-oxo-3-furanyl]-, Pyrulic acid found in *Alpinia galanga* has higher binding affinity against cancer supported targeted therapeutic protein. Phyto lipids are screened using *In silico* research, which uses Swiss ADMET, molecular docking, molecular simulations, and drug-likeness to anticipate and suggest possible hits against cancer gene targets.

Article Highlights
- Lipid ligands can be thought of as molecular targets of proteins or enzymes.
- 17-phenyl-omega-trinor-PGE2, (2E,4E,8E,10E)- dodecatetraenedioic acid, Pentanamide 3-oxo-N-[(3S)-tetrahydro-2-oxo-3-furanyl]-, Pyrulic acid - formulation of therapeutic approaches in the field of medicine traditionally.
- The molecular weight of all four selected ligands is within an acceptable range (MWT $\leq$ 500), which indicates that they can be easily absorbed, diffused, and transported according to the Lipisskis rule.

Keywords: Gas chromatography mass spectroscopy, molecular docking, EGFR, Bcl2, *Alpinia galanga*, phyto lipid ligands

Introduction
Breast cancer, the 2nd leading cause of mortality and frequently diagnosed malignancy is caused commonly by a high-fat diet, lack of physical activity and excessive alcohol intake [16]. Epidermal growth factor receptor, a first discovered ErbB family receptor tyrosine kinases and its EGFR ß signalling in the primary mammary tumour are altered in metastatic breast cancer [49]. BCL2 - an antiapoptotic protein of the BCL family expressed in various solid tumours, breast cancer, prostate cancer, colorectal cancer, lung cancer, stomach cancer, and ovarian cancer. In breast cancer, BCL2 is unregulated by the hormone oestrogens through a direct consequence of transcriptional induction [50].
In-silico study tools help to predict the active drug candidate and forecast oral bioavailability to construct suitable invigorating approaches to superintend human cancer effects. However, there have been encouraging findings regarding inhibitory processes, safety effectiveness treatment, and both Insilco and Invitro methods for locating appropriate medications from the FDA-approved drug library. Components of medicinal plants can be searched for potent therapeutic protein targets, active sites, and significant hits that will be further studied in lead optimisation and drug development to offer computational support for creating pharmaceuticals [8, 16].
Worldwide with the increase in the incidence of cancer servers like Molinspiration Cheminformatics provide tools to develop drug models or drug designs with

high-quality molecules, problem associated with cancer and molecular database tools supporting disease diagnosis [1]. solutions to a common

There is an essential requirement to develop substructure and similarity searches and this software helps to identify new and potent anticancer agents with fragment-based virtual screening, resistance problems involving the computational study of pharmacokinetic Mo inspiration tools have various parameters like bioactivity score and toxicity parameters with easily available on any online platform [2].

In silico Pharmacokinetic study of known drugs with major properties like hydrophobicity, drug-likeness (Lipinski's rule of five) in electronic distribution, and hydrogen bonding. Drug distribution throughout the body is largely influenced by hydrophobicity, which may be examined in the pharmacokinetic analysis using the tool Molinspiration. The hydrophobicity of any molecule can be evaluated in the Cheminformatics server by analysing the value of log P. big chemical following absorption [7]. Predicting the surface properties of polar molecules provides lead for functional drug development for intestinal drug absorption. The study of interaction reveals the binding of phytochemicals with amino acid residues of target proteins that medicinal plants containing these Phyto lipids like 17-phenyl-omega-trinor-PGE2, (2E, 4E, 8E, 10E)- dodecatetraenedioic acid, Pentanamide 3-oxo-N-[(3S)-tetrahydro-2-oxo-3-furanyl]-, Pyrulic acid can be used in the formulation of therapeutic approaches in the field of medicine traditionally.

This *In-silico* study of Phyto lipids 17-phenyl-omega-trinor-PGE2, (2E, 4E, 8E, 10E)-dodecatetraenedioic acid, Pentanamide 3-oxo-N-[(3S)-tetrahydro-2-oxo-3-furanyl]-, Pyrulic acid found in *Alpinia galanga* has higher binding affinity against cancer supported targeted therapeutic protein. The computer programme Auto Dock Vina 1.1.2 was used to conduct the molecular docking investigations. The online Swiss model was utilised to model the three-dimensional protein structures that were obtained from the RCSB PDB databases. Phyto lipids are screened using *In silico* research, which uses Swiss ADMET, molecular docking, molecular simulations, and drug-likeness to anticipate and suggest possible hits against cancer gene targets.

Methodology

1. Collection of sample and plant authentication

Rhizomes of *Alpinia galanga* were obtained from the farmed agricultural site in Sabarimala, near the borders of Tamil Nadu and Kerala. The source of the rhizomes was verified by the Botanical Survey of India (BSI), Southern Regional Centre, Coimbatore. The specimens' voucher number is BSI/SRC/5/23/2019/Tech/3217.

2. Preparation of Phyto lipid extracts from *Alpinia galanga*:

Alpinia galanga rhizomes were electrically blended, shade-dried, sieved, and kept at room temperature pending additional examination. The powdered samples were extracted in a Soxhlet apparatus at 60–65 °C for 48 hours using 250 cc of Methanol: Chloroform in a 2:1 ratio and 1% KCL [51]**.** The filtrate was then evaporated. Until additional examination, the resulting extracts were kept in storage at -20 °C. It was determined what percentage of the Phyto lipid extracts were produced [5].

3. Gas chromatography Mass spectrometry

Methanol was used to prepare the plant samples that had been lipid extracted for examination. Shimadzu GC-2010 (Serial No.: O20394703148) was used to obtain GC-MS spectra. Gas chromatography (GC) and mass spectrometry (MS) are two distinct analytical techniques that are combined to analyse complex organic and biochemical mixtures and separate volatile and semi-volatile compounds with high resolution, allowing for precise identification and quantification. Bypassing the sample through a stationary phase that is fixed in the column and an inert gas (mobile phase), the gas chromatography component of the process separates various compounds in the sample into pulses of pure chemicals based on their volatility. The mass spectrometer gathers compound spectra as they come out of a chromatographic column and uses this information to identify and quantify the chemicals based on their mass-to-charge ratio (m/z). For the GC/MS analysis, the lipid-extracted plant samples were produced using a 2:1 ratio of chloroform to methanol at a concentration of 1 mg/ml. Plotting was done after spectra were adjusted to the baseline blank [52].

4. Software platform for molecular modelling of selected ligands and Protein preparation

We obtained the ligand structures over the internet at PubChem (https://pubchem.ncbi.nlm.nih.gov/). The protein data bank provided the 3D crystalline structures of the antiapoptotic proteins EGFR (PDB ID:3UG2) and BCL2 (PDB ID:5AGW). The Auto Dock Tools 1.5.7 (https://ccsb.scripps.edu/mgltools/downloads/) were utilised to produce the protein and ligands. Auto Dock V 1.1.2 was used to conduct the docking investigation. The intermolecular interactions between the ligand and protein were examined using Discovery Studio and the PyMol programme(https://pymol.org/).

5. Determination of ADMET and drug-likeness prediction

Following the molecular docking investigations of Phyto lipids with two target genes for breast cancer, the online tool Swiss ADME (http://www.swissadme.ch/index.php) was used to screen Phyto lipids for absorption, distribution, metabolism, elimination, and toxicity (ADMET) to predict their pharmacokinetic features.

Molinspiration, an online program, was utilised to upload the structures of the chosen Phyto lipids in SMILES format to anticipate the features of drug-likeness. The prospective phytochemicals were selected for more research on protein-ligand interactions based on their drug-likeness and bioavailability. It is significant to note that the formula satisfying the terms lipophilicity, hydrophobicity, and polarity of the compound—which gauge the compound's capacity to bind to the target protein's hydrophobic sites—is the basis for calculating logP [9].

Results and Discussion

Gas chromatography Mass spectrometry- Retrieval of the lipid ligands: GC – MS analysis was carried out to identify the compounds present in the sample. The peaks were absorbed for the total lipid extracts of *Alpinia galanga* (Figure 1). Twenty-eight Phyto lipids (Supplementary data - Table 1) were identified from the resultant extract of *Alpinia galanga* ligands and thirteen lipid ligands (Supplementary data – Table 2) were used to the compounds decipher which will bind to

the active site of the specific target. The chemical structure, IUPAC Name, Exact mass, lipid classification and smiles of the ligands were downloaded from the LIPID MAPS Structure Database – LMSD (https://www.lipidmaps.org/databases/lmsd/overview) (Supplementary data – Table 3) and the PubChem database (https://pubchem.ncbi.nlm.nih.gov/) which contains 32000 compounds with their physical and chemical properties. The specific activity of the compounds separated was screened, and Pa and Pi values were pass-predicted using the online tool (https://www.way2drug.com/passonline/index.php). (Supplementary data – Table 4)

Table 1: Using the CASTp service, predicted active sites for proteins in their non-liganded state.

Protein PDB ID	CASTp - Active site prediction
3UG2	LEU718 LEU718 LEU718 LEU718 SER719 SER719 VAL726 VAL726 VAL726 ALA743 ALA743 ALA743 LYS745 LYS745 LYS745 LYS745 LYS745 ILE759 GLU762 MET766 CYS775 CYS775 ARG776 ARG776 LEU788 LEU788 LEU788 MET790 MET790 MET790 MET790 GLN791 GLN791 GLN791 GLN791 LEU792 MET793 MET793 MET793 MET793 MET793 MET793 PRO794 PRO794 GLY796 GLY796 CYS797CYS797 CYS797 ASP800 ASP800 ARG841 ASN842 LEU844 LEU844 LYS852 THR854 THR854 ASP855 ASP855 ASP855 ASP855 ASP855
5AGW	ASN143 ASN143 ASN143 TRP144 TRP144 TRP144 ARG146 ARG146 ARG146 ARG146 TRP188 TRP188 ASN192 ASN192 ASN192 ASN192 ASN192 GLY193 ALA197 ALA197 ALA197 GLU200 GLU200 LEU201 LEU201 LEU201 LEU201 LEU201 ALA100 ASP111 ASP111 ASP111 ASP111 GLU114 GLU114 GLU114 GLU114 GLU114 GLU114 GLU114 MET115 MET115 MET115 GLU136 ARG139 ARG139 ARG139 ASP140 ASP140 ASP140 ASP140 ASP140 ASP140 GLY141 GLY141 VAL142 VAL142 VAL142 ASN143 ASN143 TRP144 TRP144 TRP144 TRP144 TRP144 GLY145 GLY145 ARG146 ARG146 ARG146 ARG146 ARG146 VAL148 TRP188 TRP188 ASP191 ASN192 ASN192 ASN192 ASN192 ALA197 ALA197 ALA197 PHE198 PHE198 PHE198 LEU201 LEU201 LEU201 TYR202 TYR202 TYR202 TYR202 ILE3 ILE3 ILE3 ILE3 ILE3 GLN5 GLN5 GLN5 GLN5 GLN5 LEU7 ARG8 ARG8 ARG8 ARG8 ARG8 ARG8 ARG8 ILE10 ILE10 ILE10 ASP12 ASP12 ASP12 ASP12 ASP12 ASP12 PHE14 PHE14 ASN15 ASN15 ASN15 ASN15 ASN15 ASN15 ASN15 TYR18 TYR18 TYR18 ALA19 ALA19 ALA19 GLN5 GLN5 GLN5 GLN5 ARG8 ARG8 ARG8 ARG8 ARG8 ARG8 ARG8 ILE10 ASP12 ASP12 ASP12 ASP12 ASP12 ASP12 ASN15 ASN15 ASN15 ASN15 ASN15 ASN15 TYR18 ALA19 ALA19 ALA19 ARG20 ARG21 ARG21 ARG21

Table 2: Pharmacokinetic parameters of Phyto lipid compounds

Compound Name	mi LogP	TPSA	n atoms	MW	n ON	nOHNH	n violation	n rotb	Volume
Bicycle [3.1.1] heptane, 6 methyl	2.74	94.83	28	386.49	5	3	0	11	374.98
Diethyl phthalate	1.90	74.60	26	222.24	4	2	0	7	209.91
Amfetamine - M	-1.43	72.47	14	199.21	5	1	0	4	180.73
Pyrulic acid	6.43	37.30	19	264.41	2	1	1	11	290.58

Table 3: Mol-inspiration bioactivity score of selected lipid compounds

Compound Name	GPCR ligand	Ion channel modulator	Kinase inhibitor	Nuclear receptor ligand	Protease inhibitor	Enzyme inhibitor
Bicycle [3.1.1] heptane, 6 methyl	0.72	0.18	-0.19	0.52	0.33	0.55
Diethy phthalate	-0.09	0.06	-0.45	0.04	-0.21	0.18
Amfetamine - M	-0.61	-0.51	-1.34	-0.90	-0.33	-0.04
Pyrulic acid	0.30	0.57	-0.15	0.65	0.23	0.73

Selection of Breast cancer targets

In Oncology – the search for the predictors of new molecular prognostic factors and therapeutic responses was investigated intensively. Among the notable breast cancer target genes identified to BCL2 and EGFR (Table 1) (Figure 2). BCl 2 (proapoptotic or antiapoptotic protein) – intensively studied owing to their importance in signalling pathway regulation toward apoptosis, tumorigenesis, and specific cellular responses to anticancer therapeutics. BH3 protein binding functional effect with the anti-apoptotic BCL 2 family deserves more study to understand the intermolecular interactions and decipher the mysteries of cellular commitments to apoptosis [47]. Overexpression of EGFR might lead to the TNBC or IBC with the outcomes of, a larger size tumour and poor differentiation of cells. The main signalling pathways mediated by EGFR are PI3 kinase, Ras-Raf-MAPK pathway, JNK and PLCγ which control various biological functions [48]. Sequence alignment of EGFR and BCL2 protein with conserved homology domains was also determined using clustal W (https://www.genome.jp/tools-bin/clustalw) (Figure 3).

Molecular docking

Understanding the binding interactions between molecules and the amino acid residues that cause biological activity is the goal of molecular docking investigations. The protein-ligand binding process reaches an equilibrium state and stable complex through Gibbs free energy (Kcal/mol). In this study, molecular docking results indicate that *Alpinia galanga*'s Phyto lipid ligands tend to bind to EGFR and BCL2 target proteins with the lowest binding energy (Figure 5 and 6) (Table 6).

The docking scores of the four Phyto lipid ligands against each protein are summarized in Table 6. It was predicted that certain amino acid residues would be involved in binding pockets with ligand molecules. The interaction between lead inhibitors and 19 potential binding residues, as indicated in Table 1, was discovered. These residues included LEU, SER, VAL, ALA, LYS, ILE, GLU, MET, ARG, GLN, PRO, ASP, THR, ASN, TRP, GLY, PHE, and TYR. Docking features such as hydrophobicity, H-bond, ionization, aromatic compounds, and charges were calculated.

A key component of structure-based drug design is the interaction between proteins and ligands. The most reliable confirmation indicates that the free energies of binding (ΔG bind Kcal/mol) with EGFR for 17-phenyl-omega-trinor-

PGE2, (2E, 4E, 8E, 10E)-dodecatetraenedioic acid, Pyrulic acid were -6.9 Kcal/mol, -5.1 Kcal/mol, and -5.3 Kcal/mol. Similarly, the free energies of binding (⁄Gbind Kcal/mol) with BCL2 for 17-phenyl-omega-trinor-PGE2, (2E,4E,8E,10E)-dodecatetraenedioic acid, Pentanamide, 3-oxo-N-[(3S)-tetrahydro-2-oxo-3-furanyl] were -6.7 Kcal/mol, -5.3 Kcal/mol, and -4.5 Kcal/mol, respectively (Figure 5 and 6). Furthermore, docking studies provide important information on the mechanism of the reference inhibitor's binding to the active site.

Determination of *In-silico* pharmacokinetic properties, ADME and drug-likeness of selected Phyto lipid ligands

Four lipid ligands were selected out of thirteen Phyto lipid ligands, and their pharmacokinetic properties, bioactivity score, and various drug-likeness properties were analysed using SWISSADME (Table 4**).** The molecular weight of all four selected ligands is within an acceptable range (MWT $\leq$ 500), which indicates that they can be easily absorbed, diffused, and transported according to the Lipisskis rule. The MLog P value, which is used to calculate the lipophilic efficiency that measures the potency of drugs, is also in an accepted range. The hydrophobicity of the molecules was evaluated using the log P value, which plays a vital role in the drug distribution after absorption (Figure 4). The topological polar surface area (TPSA) was evaluated to analyse drug transport. Table 2 provides a detailed analysis of these pharmacokinetic parameters. Based on the bioactivity score (Table 7), lipid components with a score of more than 0.00 are biologically active, those between 0.5 to 0.00 are moderately active, and those less than -0.50 are inactive (Table 3 and Table 5). The results of this study provide a lead for the design and development of a new potent Phyto lipid drug for breast cancer. The computational study of all selected drugs provides information about their pharmacokinetics parameters, which can help in designing more effective and less toxic drugs.

Table 4: Pharmacokinetic Properties

Compound Name	LM ID	Smiles	Property							Log P
			Water solubility (log mol/L)	Caco2 permeability (log Papp in 10-6 cm/s)	Intestinal absorption (%)	Skin permeability (log Kp)	P-glycoprotein substrate	P-glycoprotein I inhibitor	P-glycoprotein II inhibitor	
Bicycle [3.1.1] heptane, 6-methyl]	LMFA03010067	[C@H]1(/C=C/[C@@H](O)CCC2C=CC=CC=2)[C@H](O)CC(=O)[C@@H]1C/C=C\CCCC(=O)O	-3.612	1.162 log Papp in 10-6 cm/s	56.93	-2.735	Yes	No	No	3.3036
Diethyl phthalate	LMFA01170008	C(/C=C/C=C/CC/C=C/C=C/C(=O)O)(=O)O	-2.311	0.737	95.042	-2.735	No	No	No	2.1606
Amfetamine - M	LMFA08030031	[C@@H]1(CCOC1=O)NC(=O)CC(=O)CC	-0.622	0.6	91.265	-3.567	No	No	No	-0.2127
Pyrulic acid	LMFA01030482	C(CCCCCCC#C/C=C/CCCCCC)(=O)O	-5.733	1.584	94.156	-2.681	No	No	No	4.9416

Table 5: Drug likeness of the ligands – SWISSADME

Properties	Molecules 1	Molecules 2	Molecules 3	Molecules 4
Physicochemical Properties				
Number of heavy atoms	27	16	14	19
Number of aromatic heavy atoms	6	0	0	0
Fraction Csp3	0.48	0.17	0.67	0.71
Number of rotatable bonds	11	7	5	11
Number of H-bond acceptors	4	4	4	2
Number of H-bond donors	2	2	1	1
Molar Refractivity	107.98	61.45	47.75	83.29
TPSA	74.60 Å²	74.60 Å²	72.47 Å²	37.30 Å²
Lipophilicity				
Log P o/w (iLOGP)	2.95	1.89	1.09	3.98
Log P o/w (XLOGP3)	2.73	2.08	0.50	6.43
Log P o/w (WLOGP)	3.42	2.16	-0.21	5.02
Log P o/w (MLOGP)	2.31	1.77	-0.47	4.23
Log P o/w (SILICOS-IT)	5.04	1.84	0.92	5.18
Consensus Log P o/w	3.29	1.95	0.36	4.97
Water Solubility				
Log S (ESOL)	-3.30	-2.07	-1.06	-4.80
Solubility	1.88-01 mg/ml; 5.07e-04 mol/l	1.91e+00 mg/ml; 8.58e-03 mol/l	1.73e+01 mg/ml; 8.71e-02 mol/l	4.15e-03 mg/ml; 1.57e-05 mol/l
Class	Soluble	Soluble	Very soluble	Moderately soluble
Log S (Ali)	-3.95	-3.28	-1.59	-7.01
Solubility	4.15e-02 mg/ml; 1.12e-04 mol/l	1.18e-01mg/ml; 5.29e-04 mol/l	5.10e+00 mg/ml; 2.56e-02 mol/l	2.60e-05 mg/ml; 9.84e-08 mol/l
Class	Soluble	Soluble	Very soluble	Poorly soluble
Log S (SILICOS-IT)	-4.38	0.20	-1.54	-4.27
Solubility	1.53e-02 mg/ml; 4.13e-05 mol/l	3.48e+02 mg/ml; 1.57e+00 mol/l	5.76e+00 mg/ml; 2.89e-02 mol/l	1.42e-02 mg/ml; 5.38e-05 mol/l

Class	Moderately soluble	Soluble	Soluble	Moderately soluble
Pharmacokinetics				
GI absorption	High	High	High	High
BBB permeant	Yes	Yes	No	Yes
P-gp substrate	Yes	No	No	No
CYP1A2 inhibitor	Yes	No	No	Yes
CYP2C19 inhibitor	No	No	No	No
CYP2C9 inhibitor	No	No	No	Yes
CYP2D6 inhibitor	No	No	No	No
CYP3A4 inhibitor	No	No	No	No
Log Kp (skin permeation)	-6.62 cm/s	-6.18 cm/s	-7.16 cm/s	-3.35 cm/s
Druglikeness				
Lipinski	Yes	Yes	Yes	Yes
Ghose	Yes	Yes	Yes	Yes
Veber	No	Yes	Yes	No
Egan	Yes	Yes	Yes	Yes
Muegge	Yes	Yes	No	No
Bioavailability Score	0.55	0.85	0.55	0.85
Medicinal chemistry				
Leadlikeness	No	No	No	No
Synthetic accessibility	4.38	3.23	2.26	3.91

ADMET- Absorption, Distribution, Metabolism, Excretion and Toxicity, TPSA – Topological polar surface area, BBB- blood-brain barrier, GI-Gastrointestinal track.

Table 6: Details of docking score of the compounds with EGFR (PDB ID: 3UG2) and Bcl2 (PDB ID: 5AGW)

S.no	Pubchem CID	Ligand Name	EGFR – Dock Score (kcal/mol)	Bcl2 - Dock Score (kcal/mol)
1	5541	Triacetin (Glycerin)	-4.9	-5.0
2	6581	Propionic acid (2-propyn-1-ol)	-3.3	-3.4
3	176	Acetic acid (Acetic acid, methyl ester)	-2.7	-3.2
4	1032	Propionic acid (Propanoic acid, 2-oxo-, methyl])	-3.2	-3.4
5	642034	Penta-2,4-dienoic acid (2-Cyclopenten-1-one, 2-hydroxy-)	-4.3	-4.2
6	54697417	3-Hydroxybut-2-enoic acid (2-Hydroxy-gamma-butyrolactone)	-4	-4.5
7	20848966	2,3-Dihydroxy-valeric acid (1,2,3-Propanetriol, monoacetate)	-4.3	-4.3
8	5283068	17-phenyl-omega-trinor-PGE2 (Bicyclo[3.1.1]heptane, 6-methyl])	-6.9	-6.7
9	9543653	(2E,4E,8E,10E)-dodecatetraenedioic acid (Diethyl phthalate)	-5.1	-5.3
10	11820073	Pentanamide, 3-oxo-N-[(3S)-tetrahydro-2-oxo-3-furanyl]- (Amfetamine-M)	-5.5 (Did not bind in target site)	-5.2
11	5312621	Pyrulic acid (Farnesyl acetate 2)	-5.3	-4.5
12	10465	Heptadecanoic acid (Heptadecanoic acid, methyl es)	-4.6	-4.6
13	985	Palmitic acid (N-Hexadecanoic acid)	-4.7	-4.4
14	Inhibitor from crystal structure 2O21	3-Nitro-N-{4-[2-(2-Phenylethyl)-1,3-Benzothiazol-5-Yl] Benzoyl}-4-{[2-(Phenylsulfanyl)Ethyl] Amino} Benzenesulfonamide	-9.1	-7.8

Table 7: Docking score and interaction of ligands with the amino acids

Selected Biomolecules (Phyto lipids)	**17-phenyl-omega-trinor-PGE2**				**(2E,4E,8E,10E)-dodecatetraenedioic acid**				**Pentanamide, 3-oxo-N-[(3S)-tetrahydro-2-oxo-3-furanyl]-**		**Pyrulic acid**	
Protein and PDB ID	**EGFR (PDB ID: 3UG2)**		**Bcl2 (PDB ID: 5AGW)**		**EGFR (PDB ID: 3UG2)**		**Bcl2 (PDB ID: 5AGW)**		**EGFR (PDB ID: 3UG2)**	**Bcl2 (PDB ID: 5AGW)**	**EGFR (PDB ID: 3UG2)**	**Bcl2 (PDB ID: 5AGW)**
Docking score of Selected biomolecules)	-6.9		-6.7		-5.1		-5.3		-5.5	-5.2	-5.3	-4.5
Nature of Interaction												
Hydrogen bonding interactions	**Amino acids**	**Distance (Å)**	**Amino acids**	**Distance (Å)**	**Amino acids**	**Distance (Å)**	**Amino acids**	**Distance (Å)**	**Amino acids**	**Distance (Å)**	**Amino acids**	**Distance (Å)**
	H···Asp111	3.4	O···Met793	2.1	H···Ala149	2.3	O···Gly796	2.8	H15···Ala743	2.9	H11···Ala149	3.2
							H24···Arg841	3.3	H14···Leu788	3.4	H01···Val133	2.8
			HO2···Thr854	2.3					O···Gln791	3.3	O···Met115	2.3
									O···Met793	2.3		
Hydrophobic interactions	Lig···Phe112 (Pi-Pi Stacked ···Pi orbital)	3.4	Lig···Leu718 (Pi sigma···Pi orbital)	3.8	Lig···Tyr108 (Pi-Alkyl···Pi-orbital)	4.3	Lig···Leu718 (Alkyl···Alkyl)	4.8	Lig···Leu718 (Alkyl···Alkyl)	4.2	Lig···Phe112 (Pi-Alkyl···Pi-orbital)	3.6
					Lig···Phe112 (Pi-Alkyl···Pi-orbital)	5.3	Lig···Val726 (Alkyl···Alkyl)	5.0	Lig···Val726 (Alkyl···Alkyl)	4.8	Lig···Val133 (Alkyl···Alkyl)	3.9
	Lig···Met115	5.0	Lig···Leu844	5.0	Lig···Phe194	4.8	Lig···Ala743	3.9	Lig···Ala743	3.9	Lig···Leu137	4.2

	(Alkyl⋯Alkyl)		(Alkyl⋯Alkyl)		(Pi-Alkyl⋯Pi-orbital)		(Alkyl⋯Alkyl)		(Alkyl⋯Alkyl)		(Alkyl⋯Alkyl)	
							Lig⋯Leu844 (Alkyl⋯Alkyl)	5.1	Lig⋯Lys745 (Alkyl⋯Alkyl)	4.3	Lig⋯Ala149 (Alkyl⋯Alkyl)	5.1
									Lig⋯Met790 (Alkyl⋯Alkyl)	4.2		

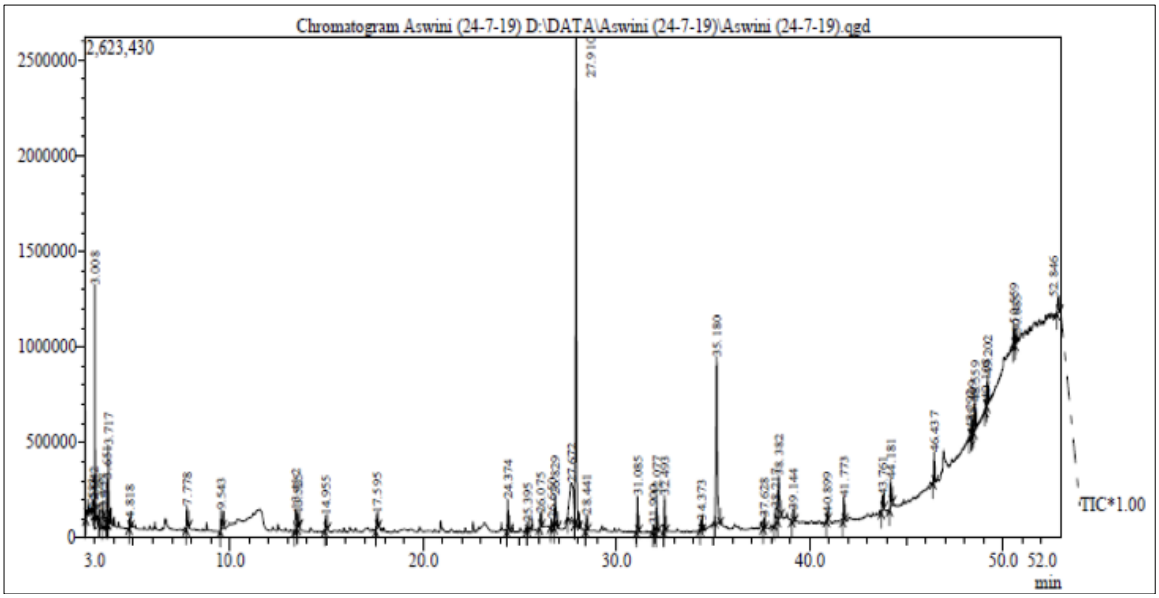

Fig 1: Chromatogram – Mass spectrum of *Alpinia galanga* (extracted Phyto lipid sample)

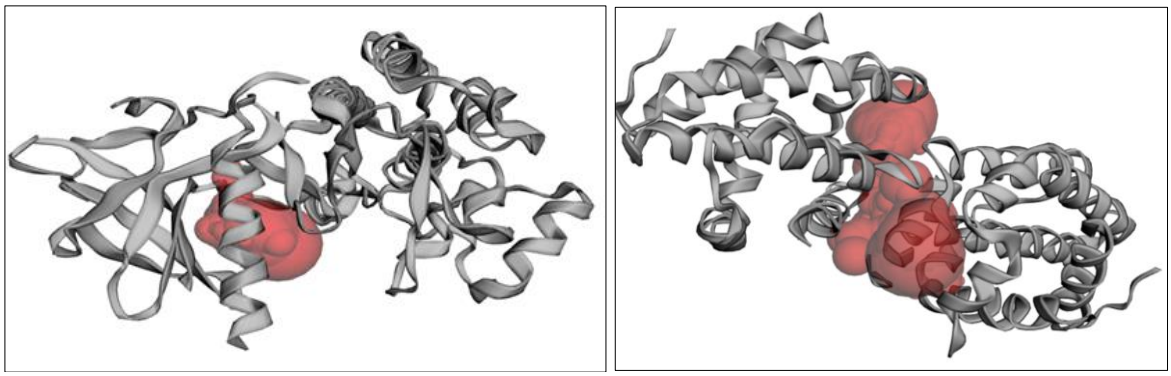

A. **B.**

Fig 2: Active site - Target gene EGFR and BCL2

```
CLUSTAL O(1.2.4) multiple sequence alignment


3UG2_1|Chain        ----GAMGIRSGEAPNQALLRILKETEFKKIKVLSSGAFGTVYKGLWIPEGEKVKIPVAI 56
5AGW_1|Chains       MAHAGRTGYDNREI----VMKYI---H----------YKLSQRGYEWDAGDDVE----- 37
5AGW_2|Chains       ------------------------------------------------------------ 0


3UG2_1|Chain        KELREATSPKAN-KEILDEAYVMASVDNPHVCRLLGICLTSTVQLIMQLMPFGCLLDYVR 115
5AGW_1|Chains       -ENRT-EAPEGTESEVVHL-----------------------------------TLR 57
5AGW_2|Chains       ------------XIXIAQ-----------------------------------XLR 9
                                    :                                    :*


3UG2_1|Chain        EHKDNIGSQYLLNWCVQIAKGMNYLEDRRLVHRDLAARNVLVKTPQHVKITDFGLAKLLG 175
5AGW_1|Chains       QAGDDFSRRYR----------------------RDFAE------MSSQLHLTPFTARGRFA 90
5AGW_2|Chains       XIGDXFNXYYA----------------------RR-------------------------- 22
                       * :.  *                       *


3UG2_1|Chain        AEEKEYHAEGGKVPIKWMALESILHRIYTHQSDVWSYGVTVWELMTFGSKPYDGIPASEI 235
5AGW_1|Chains       ---------------------TVVEELFR-DGVNWGRIVAF---FEFGGVMCV------- 118
5AGW_2|Chains       ------------------------------------------------------------ 22


3UG2_1|Chain        SSILEKGERLPQPPICTIDVYM-----IMVKCWMIDADSRPKFRELIIEFSKMARDPQRY 290
5AGW_1|Chains       ----ESVNREMSPLVDNIALWMTEYLNRHLHTWIQDNGGWDAFVELYGPSMR-------- 166
5AGW_2|Chains       ------------------------------------------------------------ 22


3UG2_1|Chain        LVIQGDERMHLPSPTDSNFYRALMDEEDMDDVVDADEYLIPQQG 334
5AGW_1|Chains       ---------------------------------------------- 166
5AGW_2|Chains       ---------------------------------------------- 22
```

Fig 3: Sequence alignment of EGFR and BCL2 protein according to clustalW with conserved homology domains

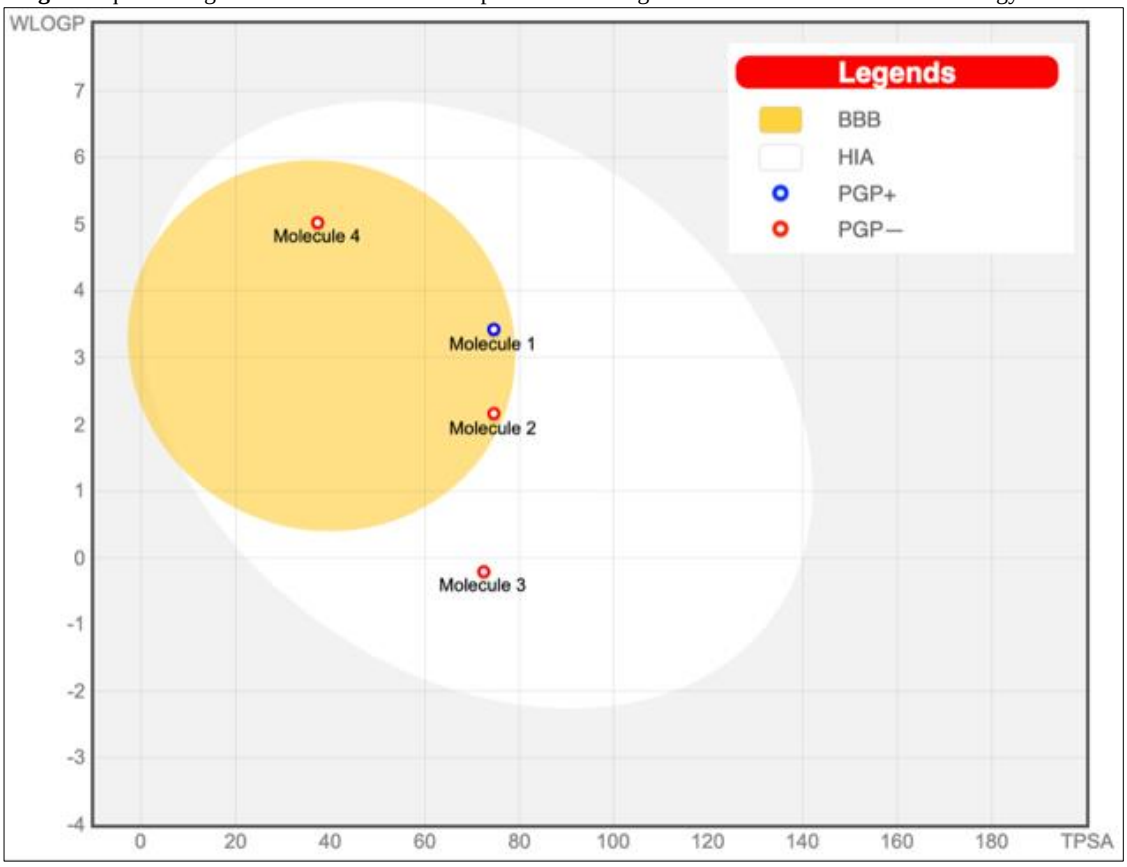

Fig 4: Pharmacokinetics Boiled egg

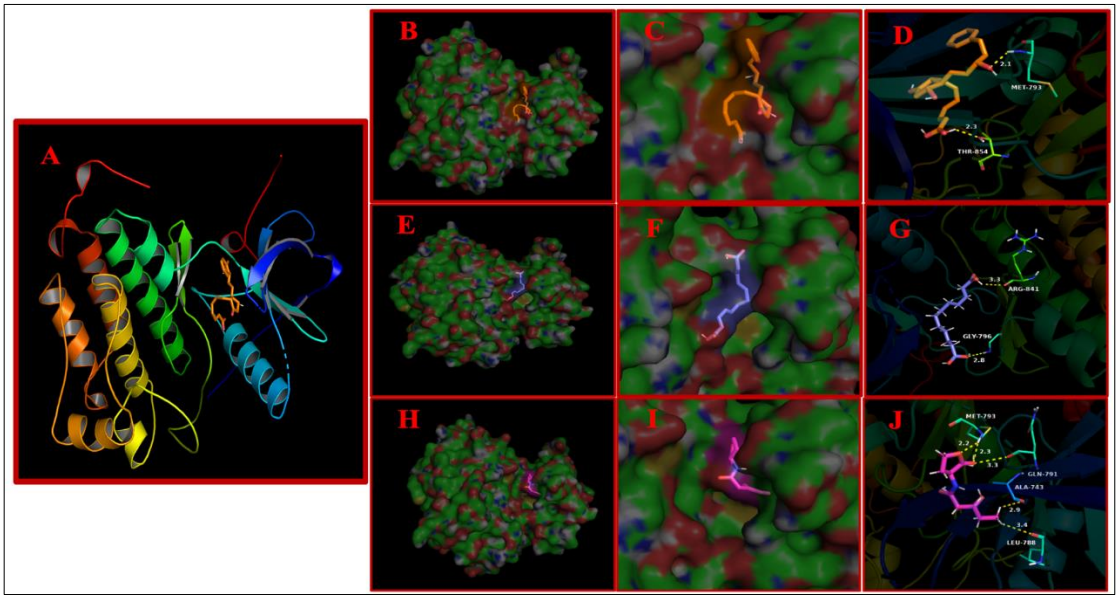

Fig 5: Molecular docking of selected lipid ligands with EGFR as a target protein

Figure 5: Molecular docking of selected lipid ligands with EGFR as a target protein: A. 2D structure of the EGFR protein, B. 3D binding mode of designed molecule in the active pockets of the EGRF receptors and 17-phenyl-omega-trinor-PGE2, C. 3D binding mode of designed molecule in the active pockets of the EGRF receptors and 17-phenyl-omega-trinor-PGE2, D. 2D binding mode of designed molecule in the active pockets of the EGRF receptors and 17-phenyl-omega-trinor-PGE2, E. 3D binding mode of designed molecule in the active pockets of the EGRF receptors and (2E,4E,8E,10E)-dodecatetraenedioic acid, F. 3D binding mode of designed molecule in the active pockets of the EGRF receptors and (2E,4E,8E,10E)-dodecatetraenedioic acid, G. 2D binding mode of designed molecule in the active pockets of the EGRF receptors and (2E,4E,8E,10E)-dodecatetraenedioic acid, H. 3D binding mode of designed molecule in the active pockets of the EGRF receptors and Pyrulic acid, I. 3D binding mode of designed molecule in the active pockets of the EGRF receptors and Pyrulic acid, J. 2D binding mode of designed molecule in the active pockets of the EGRF receptors and Pyrulic acid.

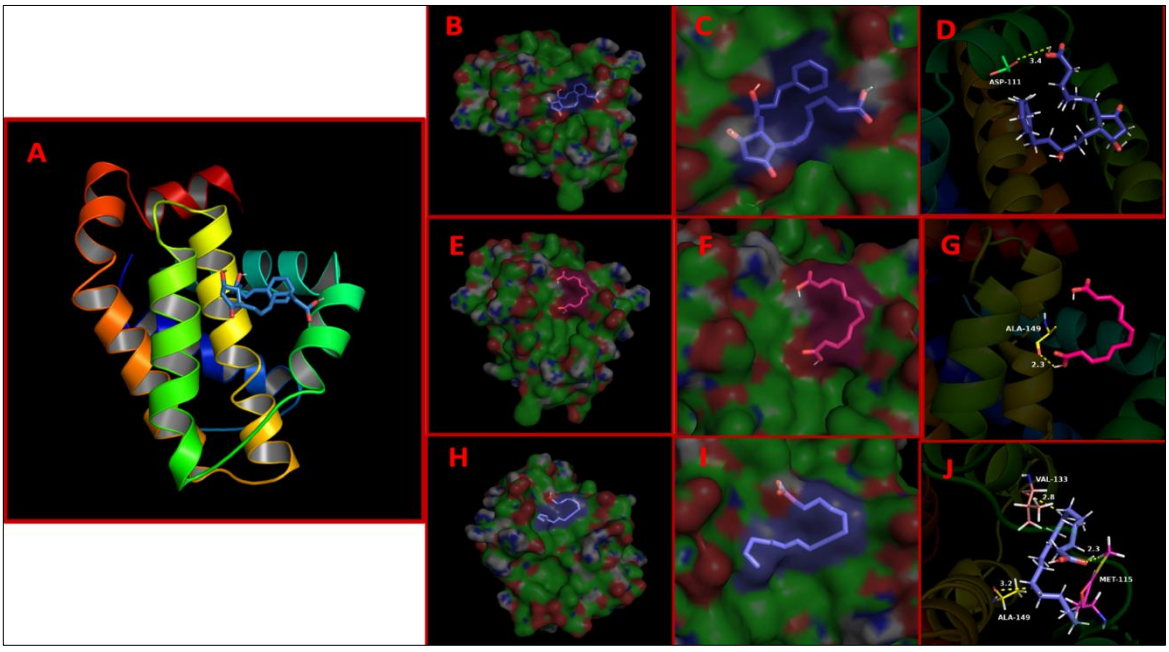

Fig 6: Molecular docking of selected lipid ligands with BCL2 as a target protein

Figure 6: Molecular docking of selected lipid ligands with BCL2 as a target protein: A. 2D structure of the BCL2 protein, B. 3D binding mode of designed molecule in the active pockets of the BCL2 receptors and 17-phenyl-omega-trinor-PGE2, C. 3D binding mode of designed molecule in the active pockets of the BCL2 receptors and 17-phenyl-omega-trinor-PGE2, D. 2D binding mode of designed molecule in the active pockets of the BCL2 receptors and 17-phenyl-omega-trinor-PGE2, E. 3D binding mode of designed molecule in the active pockets of the BCL2 receptors and (2E,4E,8E,10E)-dodecatetraenedioic acid, F. 3D binding mode of designed molecule in the active pockets of the BCL2 receptors and (2E,4E,8E,10E)-dodecatetraenedioic acid, G. 2D binding mode of designed molecule in the active pockets of the BCL2 receptors and (2E,4E,8E,10E)-dodecatetraenedioic acid, H. 3D binding mode of designed molecule in the active pockets

of the BCL2 receptors and Pentanamide, 3-oxo-N-[(3S)-tetrahydro-2-oxo-3-furanyl]-, I. 3D binding mode of designed molecule in the active pockets of the BCL2 receptors and Pentanamide, 3-oxo-N-[(3S)-tetrahydro-2-oxo-3-furanyl]-, J. 2D binding mode of designed molecule in the active pockets of the BCL2 receptors and Pentanamide, 3-oxo-N-[(3S)-tetrahydro-2-oxo-3-furanyl].

Summary and Conclusion

In 2016, Shashank Mishra and associates conducted research on the *In-silico* calculation of anti-tubercular drug ADME, bioactivity, and toxicity parameters. Among the several pharmacokinetic characteristics, tuberculosis continues to be the most common physicochemical descriptor [1]. According to estimates from the World Health Organisation, there are between 8 and 10 million new cases of tuberculosis each year. The disease COVID-19 is caused by the severe acute respiratory syndrome coronavirus 2 (SARS-CoV-2), which is the subject of extensive ongoing research to develop suitable therapeutic approaches to control its effects. Seshu Sahoo (2020) reported on an *In-silico* ADMET and molecular docking study on searching potential inhibitors from limonoids and triterpenoids for COVID-19. A combination of computational and experimental methods is utilised to find appropriate medications from the database of FDA-approved medications and medications undergoing clinical trials. The phytochemical limonin, which is known to inhibit the replication of retroviruses like HTLV-I and HIV-1, demonstrated a higher dock score towards the protein targets RdRp and ACE2, according to a recent molecular docking study on the search for COVID-19 inhibitors. *In silico* ADMET and drug-likeness prediction were used to propose potential hits against the five therapeutic protein targets of SARS-CoV-2, which are 3CLpro, PLpro, RdRp, SpG-RBD, and ACE2.

Drug development is greatly aided by ligand-receptor interactions, which are crucial in eliciting biological responses. The study examined and compared the relative affinities of 17-phenyl-omega-trinor-PGE2, (2E,4E,8E,10E)-dodecatetraenedioic acid, Pentanamide 3-oxo-N-[(3S)-tetrahydro-2-oxo-3-furanyl]-, and Pyrulic acid lipid ligands with two target proteins.

The study of ligand binding affinities with proteins can benefit from the application of molecular docking experiments. The goal of this work was to investigate ligand-receptor interactions through the application of biochemical and bioinformatic methods. Utilising bioinformatic methods, the tiny atomic interactions between the protein and ligand were examined. Potential ligands for two proteins (3UG2 and 5AGW) were looked for. The strong binding affinities of the eight lipid ligands were compared, and the bound interaction was examined to see the microscopic atomic interactions between the ligands and proteins. Pymol and other bioinformatic techniques were utilised to investigate the bound interactions between proteins and ligands. The results of the analysis were converted into pictures that show the target ligands-protein interaction.

The discovery that naturally occurring lipid ligands represent a novel class of putative ligands for physiologically important proteins is the study's primary contribution. Many details on these lipid ligands and proteins have been made public by this research. Interestingly, similar bingeing affinities and favourable binding contacts have been demonstrated by the 17-phenyl-omega-trinor-PGE2, (2E,4E,8E,10E)-dodecatetraenedioic acid, Pentanamide 3-oxo-N-[(3S)-tetrahydro-2-oxo-3-furanyl]-, and pyrulic acid groups of lipid ligands. The fundamental information about the strength of binding between lipid ligands and proteins is provided by binding affinity. To investigate the significance of the lipid-protein interaction—which has some limitations because the outcomes depend on the structure of the ligand and receptor—more information about the atomic interaction between the lipid and protein should be known. Lipid ligands can be thought of as molecular targets of proteins or enzymes.

Abbreviations

BCL2 - B-cell lymphoma 2
FDA - Food and Drug Administration
EGFR - Epidermal growth factor receptor
ErbB - Erythroblastic leukaemia viral oncogene homologue
RCSB - Research Collaboratory for Structural Bioinformatics
PDB - Protein Data Bank
ADMET - Absorption, Distribution, Metabolism, Excretion and Toxicity
GCMS - Gas chromatography Mass Spectrometry
KCL - Potassium chloride
ADME - Absorption, Distribution, Metabolism and Excretion.
NCBI - National centre for Biotechnology Information.
BSI - Botanical survey of India
NIH - National Institutes of Health
TNBC - Triple negative breast cancer
IBC - Inflammatory breast cancer
MW - Molecular weight

Conflict of interest

No financial or commercial tie might be seen as a possible conflict of interest while the research was done.

Data availability

The authors confirmed that the data supporting the findings of this study are available within the article and its supplementary materials. Raw data that supports the findings of this study are available from the corresponding author upon reasonable request.

Reference

1. Mishra SS, Sharma CS, Singh HP, Pandiya H, Kumar N. *In silico* ADME, Bioactivity and Toxicity Parameters Calculation of Some Selected Anti-Tubercular Drugs. International Journal of Pharmaceutical and Phytopharmacological Research. 2016;6(6):77. https://doi.org/10.24896/eijppr.2016661
2. Tomioka H, Namba K. Development of antituberculosis drugs: current status and future prospect. KEKKAKU: [Tuberculosis]. 2006;81(12):753-774.
3. Sharma CS, Mishra SS, Singh HP, Kumar N. *In silico* ADME and Toxicity Study of Some Selected Antineoplastic Drugs. International Journal of Pharmaceutical Sciences and Drug Research. 2016;8(1):65-67.
4. Abraham DJ. Burger's Medicinal Chemistry and Drug Discovery Volume 5: Chemotherapeutic Agents. 6th ed. John Wiley & Sons; c2003.
5. Aswini M, Kavitha Bagya S. Phytoconstituent analysis of *Alpinia galanga* and *Zingiber officinale* plant lipids - A Comparative approach. International Journal of Science & Engineering Development Research. 2022;7(8):647-654. Available from: http://www.ijrti.org/papers/IJRTI2208114.pdf

6. Palm K, Stenberg P, Luthman K, Artursson P. Polar molecular surface properties predict the intestinal absorption of drugs in humans. Pharmaceutical Research. 1997;14(5):568-571.
7. Vardhan S, Sahoo SK. *In silico* ADMET and molecular docking study on searching potential inhibitors from limonoids and triterpenoids for COVID-19. Computers in Biology and Medicine. 2020;124:103936. https://doi.org/10.1016/j.compbiomed.2020.103936
8. Vardhan S, Sahoo SK. Searching Inhibitors for Three Important Proteins of COVID-19 through Molecular Docking Studies. 2020. arXiv:2004.08095.
9. Trott O, Olson AJ. Auto Dock Vina: improving the speed and accuracy of docking with a new scoring function, efficient optimization, and multithreading. Journal of Computational Chemistry. 2010;31(2):455-461.
10. ScienceDirect. Lipophilicity. Available from: https://www.sciencedirect.com/topics/immunology-and-microbiology/lipophilicity
11. Ali R, Wendt MK. The paradoxical functions of EGFR during breast cancer progression. Signal Transduction and Targeted Therapy. 2017;2(1):16042. https://doi.org/10.1038/sigtrans.2016.42
12. Hashmi AA, Naz S, Hashmi SK, Irfan M, Hussain ZF, Khan EY, Asif H, Faridi N. Epidermal growth factor receptor (EGFR) overexpression in triple-negative breast cancer: association with clinicopathologic features and prognostic parameters. Surgical and Experimental Pathology. 2019;2(1):6. https://doi.org/10.1186/s42047-018-0029-0
13. Acharya R, Chacko S, Bose P, Lapenna A, Pattanayak SP. Structure-Based Multitargeted Molecular Docking Analysis of Selected Furanocoumarins against Breast Cancer. Scientific Reports. 2019;9(1):11103. https://doi.org/10.1038/s41598-019-52162-0
14. Laskowski RA, Jabłońska J, Pravda L, Vařeková RS, Thornton JM. PD Bsum: Structural summaries of PDB entries. Protein Science. 2018;27(1):129-134. https://doi.org/10.1002/pro.3289
15. Sohrab SS, Kamal MA. Screening, Docking, and Molecular Dynamics Study of Natural Compounds as an Anti-HER2 for the Management of Breast Cancer. Life. 2022;12(11):1729. https://doi.org/10.3390/life12111729
16. Song X, Liu Z, Yu Z. EGFR Promotes the Development of Triple Negative Breast Cancer Through JAK/STAT3 Signalling. Cancer Management and Research. 2020;12:703-717. https://doi.org/10.2147/cmar.s225376
17. Tutumlu G, Dogan B, Avsar T, Orhan MD, Calis S, Durdagi S. Integrating Ligand and Target-Driven Based Virtual Screening Approaches With *In vitro* Human Cell Line Models and Time-Resolved Fluorescence Resonance Energy Transfer Assay to Identify Novel Hit Compounds Against BCL-2. Frontiers in Chemistry. 2020;8:167. https://doi.org/10.3389/fchem.2020.00167
18. Masuda H, Zhang D, Bartholomeusz C, Doihara H, Hortobagyi GN, Ueno NT. Role of epidermal growth factor receptor in breast cancer. Breast Cancer Research and Treatment. 2012;136(2):331-345. https://doi.org/10.1007/s10549-012-2289-9
19. Inao T, Iida Y, Moritani T, Okimoto T, Tanino R, Kotani H, Harada M. Bcl-2 inhibition sensitizes triple-negative human breast cancer cells to doxorubicin. Oncotarget. 2018;9(39):25545-25556. https://doi.org/10.18632/oncotarget.25370
20. Binder C, Marx D, Overhoff R, Binder L, Schauer A, Hiddemann W. Bcl-2 protein expression in breast cancer in relation to established prognostic factors and other clinicopathological variables. Annals of Oncology. 1995;6(10):1005-1010. https://doi.org/10.1093/oxfordjournals.annonc.a059064
21. Guo P, Pu T, Chen S, Qiu Y, Zhong X, Zheng H. Breast cancers with EGFR and HER2 co-amplification favor distant metastasis and poor clinical outcome. Oncology Letters. 2017;14(6):6897-6904. https://doi.org/10.3892/ol.2017.7055
22. Arsianti A, Fadilah F, Erlina L, Paramita RI. Molecular Docking of Antimycin A3 Analogs and its Aromatic Segments as Inhibitors of Apoptosis Protein Marker Bcl-XL and Mcl-1. Asian Journal of Pharmaceutical and Clinical Research. 2017;10(8):317. https://doi.org/10.22159/ajpcr.2017.v10i8.18165
23. Abdullahi SH, Uzairu A, Shallangwa GA, Uba S, Umar AB. *In-silico* activity prediction, structure-based drug design, molecular docking and pharmacokinetic studies of selected quinazoline derivatives for their antiproliferative activity against triple negative breast cancer (MDA-MB231) cell line. Bulletin of the National Research Centre. 2022;46(1):69. https://doi.org/10.1186/s42269-021-00690-z
24. Krishna S, Kumar SB, Murthy TPK, Murahari M. Structure-based design approach of potential BCL-2 inhibitors for cancer chemotherapy. Computers in Biology and Medicine. 2021;134:104455. https://doi.org/10.1016/j.compbiomed.2021.104455
25. Taghizadeh MS, Niazi A, Moghadam A, Afsharifar A. Experimental, molecular docking and molecular dynamic studies of natural products targeting overexpressed receptors in breast cancer. PLOS ONE. 2022;17(5)
26. . https://doi.org/10.1371/journal.pone.0267961
27. Joshi C, Chaudhari A, Joshi C, Joshi M, Bagatharia S. Repurposing of the herbal formulations: molecular docking and molecular dynamics simulation studies to validate the efficacy of phytocompounds against SARS-CoV-2 proteins. Journal of Biomolecular Structure and Dynamics. 2021;40(18):8405-8419. https://doi.org/10.1080/07391102.2021.1922095
28. Huang X, Zhang Q, Wang N. The significance of Bcl-2 expression in breast cancer: A 10-year follow-up study. Journal of Clinical Investigation and Studies. 2021;4(1):127. https://doi.org/10.15761/jcis.1000127
29. Eom YH, Kim HS, Lee A, Song BJ, Chae BJ. BCL2 as a Subtype-Specific Prognostic Marker for Breast Cancer. Journal of Breast Cancer. 2016;19(3):252. https://doi.org/10.4048/jbc.2016.19.3.252
30. Han Y, Zhang J, Hu CQ, Zhang X, Ma B, Zhang P. *In silico* ADME and Toxicity Prediction of Ceftazidime and Its Impurities. Frontiers in Pharmacology. 2019;10:434. https://doi.org/10.3389/fphar.2019.00434
31. Kim A, Jang MH, Lee SJ, Bae YK. Mutations of the Epidermal Growth Factor Receptor Gene in Triple-Negative Breast Cancer. Journal of Breast Cancer. 2017;20(2):150. https://doi.org/10.4048/jbc.2017.20.2.150
32. Maennling AE, Tur MK, Niebert M, Klockenbring T, Zeppernick F, Gattenlöhner S. Molecular Targeting Therapy against EGFR Family in Breast Cancer: Progress and Future Potentials. Cancers. 2019;11(12):1826. https://doi.org/10.3390/cancers11121826

33. Kong R, Yang G, Xue R, Liu M, Wang F, Hu J. COVID-19 Docking Server: A meta server for docking small molecules, peptides and antibodies against potential targets of COVID-19. Bioinformatics. 2020;36(20):5109-5111. https://doi.org/10.1093/bioinformatics/btaa645
34. Lindeman GJ, Visvader JE. Targeting BCL-2 in breast cancer: exploiting a tumor lifeline to deliver a mortal blow? Breast Cancer Management. 2013;2(1):1-4. https://doi.org/10.2217/bmt.12.60
35. Teng YH, Tan WJ, Thike AA, Cheok PY, Tse GM, Wong NS, Yip GW, Bay BH, Tan PH. Mutations in the epidermal growth factor receptor (EGFR) gene in triple negative breast cancer: Possible implications for targeted therapy. Breast Cancer Research. 2011, 13(2). https://doi.org/10.1186/bcr2857
36. Narayanan Nair D, Padmavathy S. Molecular Docking Studies of Phytocompounds from *Aloe vera* (L.) Burm. f. having Anticancer Property, against an Antiapoptotic Bcl-2 Protein. Biosciences, Biotechnology Research Asia. 2017;14(4):1449-1456. https://doi.org/10.13005/bbra/2590
37. Dharmalingam K. Molecular docking analysis of penta galloyl glucose with the bcl-2 family of anti-apoptotic targets. Bioinformation. 2021;17(10):861-865. https://doi.org/10.6026/97320630017861
38. Ponnulakshmi R. Molecular docking analysis of Bcl-2 with phytocompounds. Bioinformation. 2020;16(6):468-473. https://doi.org/10.6026/97320630016468
39. Sultana R. Molecular docking based virtual screening of the breast cancer target NUDT5. Bioinformation. 2019;15(11):784-789. https://doi.org/10.6026/97320630015784
40. Pandi S, Kulanthaivel L, Subbaraj GK, Rajaram S, Subramanian S. Screening of Potential Breast Cancer Inhibitors through Molecular Docking and Molecular Dynamics Simulation. BioMed Research International. 2022;2022:3338549. https://doi.org/10.1155/2022/3338549
41. Hu Z, Zou X, Qin S, Li Y, Wang H, Yu H. Hormone receptor expression correlates with EGFR gene mutation in lung cancer in patients with simultaneous primary breast cancer. Translational Lung Cancer Research. 2020;9(2):325-336. https://doi.org/10.21037/tlcr-20-513.
42. DeLano WL. PyMOL: An Open-Source Molecular Graphics Tool. DeLano Scientific; c2002.
43. Majumder R, Mandal M. Screening of plant-based natural compounds as a potential COVID-19 main protease inhibitor: An *In silico* docking and molecular dynamics simulation approach. Journal of Biomolecular Structure and Dynamics. 2020;40(2):696-711. https://doi.org/10.1080/07391102.2020.1817787.
44. Nimgampalle M, Devanathan V, Saxena A. Screening of Chloroquine, Hydroxychloroquine and its derivatives for their binding affinity to multiple SARS-CoV-2 protein drug targets. Journal of Biomolecular Structure and Dynamics. 2020;39(14):4949-4961. https://doi.org/10.1080/07391102.2020.1782265.
45. Binder C, Marx D, Binder L, Schauer A, Hiddemann W. Expression of Bax in relation to Bcl-2 and other predictive parameters in breast cancer. Annals of Oncology. 1996;7(2):129-133. https://doi.org/10.1093/oxfordjournals.annonc.a010538.
46. Shah B, Modi P, Sagar SR. *In silico* studies on therapeutic agents for COVID-19: Drug repurposing approach. Life Sciences. 2020;252:117652. https://doi.org/10.1016/j.lfs.2020.117652.
47. Youle R, Strasser A. The BCL-2 protein family: opposing activities that mediate cell death. Nature Reviews Molecular Cell Biology. 2008;9(1):47-59. https://doi.org/10.1038/nrm2308.
48. Masuda H, Zhang D, Bartholomeusz C, Doihara H, Hortobagyi GN, Ueno NT. Role of epidermal growth factor receptor in breast cancer. Breast Cancer Research and Treatment. 2012;136(2):331-345. https://doi.org/10.1007/s10549-012-2289-9.
49. Bibi I, Djelouah K, Remah A, Afechtal M. Pepino Mosaic Virus: a serious threat to tomato crops worldwide. Revue Marocaine des Sciences Agronomiques et Vétérinaires. 2017;5:231-237.
50. Yong WS, Hsu FM, Chen PY. Profiling genome-wide DNA methylation. Epigenetics & Chromatin. 2016;9:1-6.
51. Bligh EG, Dyer WJ. A rapid method of total lipid extraction and purification. Canadian Journal of Biochemistry and Physiology. 1959;37(8):911-917.
52. Liu ZK, Zhou B, Zhang Y, Wang ZJ, Weng HM, Prabhakaran D. Discovery of a three-dimensional topological Dirac semimetal, Na3Bi. Science. 2014;343(6173):864-867.